Journal of Metals, Materials and Minerals. Vol. 13 No.2 pp. 25-31, 2004.

STRESS EVOLUTION IN NICKEL BASED SINGLE CRYSTAL SUPERALLOY SUBJECTED TO THERMAL CYCLING

Jozef ZRNÍK[1*], Peter JENČUŠ[2], Petr LUKÁŠ[2], Peter HORŇAK[1] and Panyawat WANGYAO[3]

[1]Department of Materials Science, Faculty of Metallurgy, Technical University of Košice, Slovak Rep.

[2]Institute of Nuclear Physics, Řež near Prague, Czech Rep.

[3]Metallurgy and Materials Science Research Institute, Chulalongkorn University, Bangkok, Thailand

ABSTRACT

The deformation behaviour of single crystal nickel based superalloy CM 186LC has been evaluated in conditions of variable temperature. Deformation changes resulting from continuous thermal transients performed at a temperature interval of 50°C to 950°C were recorded on line. The number of thermal transient tests was conducted, applying a different maximum number of cycles in each test. The resulting strain, in a transverse direction to the gauge length was measured. The stresses incurred in the specimen were calculated using the recorded strains and the coefficient of thermal expansion of nickel based single crystal superalloy CM 186LC, which was specifically measured for this alloy. The stress-strain characteristics were calculated as a function of temperature and thermal cycles applied. Neutron diffraction analysis was used to investigate the microstrain development in the two phases that the alloy consisted of.

Keywords : Nickel superalloy, structure, thermal fatigue, thermal expansion, strain, stress, neutron diffraction.

* To whom correspondence should be addressed:
E-mail: jozef.zrnik@tuke.sk; jzrnik@comtesfht.cz

INTRODUCTION

Thermal fatigue is a result of steep temperature gradients in a component or across a section and can occur in a perfectly homogeneous isotropic material as well as in a multiphase structure. However, thermal fatigue damages can develop even under condition of uniform specimen temperature when internal constraints arise due to various thermal expansion mismatch coefficients of the phases that the alloy consists of. The constraints due to repeated thermal transients can reach an inelastic strain range. Examples of thermal fatigue can be found wherever the structures or component assembly undergo thermal loading. Turbine engines are exposed to cyclic high temperature operation. The respective straining of the material leads to crack initiation and crack propagation. Potential failure modes for gas turbine parts are high and low cycle fatigue, creep, thermal fatigue. An improved durability of hot section components has been achieved by a better understanding of the component behaviour under both thermal and mechanical loading. Therefore, the thermal fatigue phenomenon would have been considered in studies of deformation and damage evolution at thermal exposure loading schedules.

The thermal fatigue studies have been conducted in different nickel based superalloys, including cast, wrought, and directionally solidified structures, evaluating the thermal fatigue damage mechanisms under various testing conditions (Lukas, *et al.* 1998; and Kasik, *et al.* 1998). Under thermal fatigue conditions considerable changes in nickel based superalloys structure have been known to occur, including the size and morphology of gamma prime and formation of dislocation networks around precipitates (Blumm, *et al.* 1995; and Malpertu, *et al.* 1990).

In the present paper, the special attention is paid to the thermal fatigue of single crystal nickel based superalloy CM186 LC. The study was to provide information on fundamental aspects of the strain resulting in specimens subjected to applying a different maximum number of thermal cycles in each test. The stresses incurred in specimen are calculated using the recorded strains and temperature dependences of stress were plotted. High Resolution Neutron Diffraction (HRND) analysis was used to evaluate and quantify the microstrain resulting in the CM186LC single crystal superalloy due to a constrained lattice mismatch on the gamma matrix and gamma prime interface in dependence of the number of transients in the thermal fatigue test.

EXPERIMENTAL PROCEDURE

Single crystal (SX) nickel based superalloy CM186LC is the result of applying single crystal casting technology, and originally designed to improve the castability and yield of complex directionally solidified columnar aerofoil segments that are typically used in turbine vane applications. Nominal composition of the SX superalloy CM186LC is given in Table 1.

The specimens in the form of rods 150 mm long and 10 mm in diameter were directionally solidified at ABB Alstom, UK. To obtain a range of dendrite arm spacing in samples growth rates in the range 1-30 mm min^{-1} and gradients up to 13 K mm^{-1} were employed. The crystallography orientation data of individual bars are stated in (Zrnik and Hornak, 2000). For the structural investigation the light microscopy, scanning electron microscopy (SEM), and transmission electron microscopy (TEM) of thin foils were used.

Table 1 Chemical composition of CM186LC SX nickel based superalloy.

Element	C	Cr	Co	Mo	W	Al	Ti	Ta	Re	B	Zr	Hf	Ni
wt. pct	0.069	6.0	9.3	0.5	8.4	5.7	0.7	3.4	2.9	0.015	0.006	1.4	Bal

Thermal fatigue tests have been carried out on cylindrical specimens machined from 10 mm diameter SX CM186LC bars. The gauge section of the specimen has a thin rectangular cross section in order to obtain a uniform temperature during thermal cycling. The specimen designed for the thermal cycling test is presented in Figure 1. The specimen is heated by resistance heating for 45 seconds until the maximum temperature of 950°C is reached, followed by nitrogen gas cooling for 15 seconds down to a minimum temperature of 50°C. The resulting strain, in transverse direction to the gauge length was measured with a contact extensometer. A number of thermal fatigue tests (up to 1000 cycles) were conducted, applying a different maximum number of cycles in each test. The stresses incurred in the specimen are calculated using the recorded strains and the coefficient of thermal expansion of SX CM186LC. The tests were carried out on as-cast specimens and the obtained stress-temperature cycles were found.

The high resolution neutron diffraction technique was applied in investigation of microstrain originated in nickel based superalloy due to applied thermal fatigue cycling. The specimens exposed to different number of thermal cycles were tested at high resolution diffractometer G5.2 (LLB Saclay) and verified at SPN-100 (INF Rez near Prague). The 200 diffraction profiles at the neutron wavelength of λ = 2.86 Å were recorded and their evolution with applied thermal loading was then analyzed.

EXPERIMENTAL RESULTS AND DISCUSSION

Microstructure

The microstructure analysis was carried out on transversal sections of the bar at two positions. The as-cast microstructure of SX CM186LC consists of a eutectic gamma/gamma prime structure (in interdendritic regions) surrounded by the primary gamma with a finely precipitated gamma prime phase (in dendrites). An example of the dendritic structure is shown in Figure 1. This is micrograph obtained on the transverse section (i.e. section n perpendicular to [001] direction) of the HOWMET ltd. solid bar.

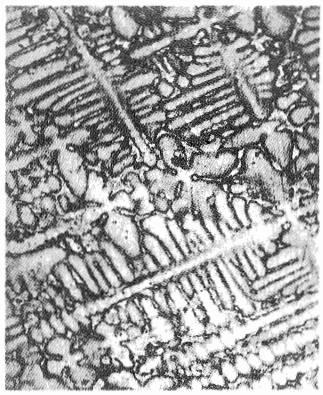

Figure 1 Micrograph of 'virgin' dendritic structure of cast bar.

Results of dendritic structure analysis confirmed some variation of the secondary dendrite arms length among the different specimens and sections (Cyrska-Filemonowiez and Dubiel, 2000). In light microscope the overall appearance of the gamma/gamma prime morphology emerges when the higher magnification is used, Figure 2. In dendrites arms the gamma prime precipitates appear homogeneous. The morphology of the phases

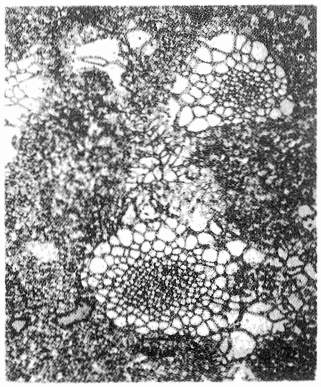

Figure 2 Micrograph of eutectic pools.

of the alloy was distinguished better by SEM structure analysis. The SEM micrograph shown in Figure 3 highlights the heterogeneous

gamma/gamma prime structure in SX as-cast alloy. The eutectic gamma/gamma prime in SX alloy is highly irregular with gamma prime particles reaching a maximum width in excess of 10 μm. Between coarse eutectic pools and 'regular' dendritic structure there is a transition region where gamma prime precipitates are

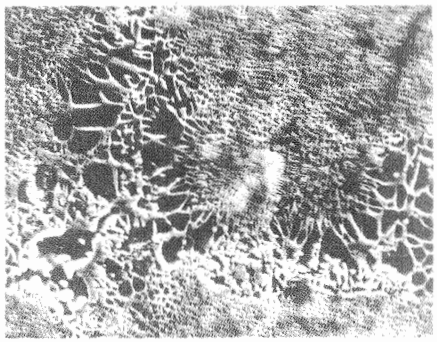

Figure 3 SEM micrograph of interdendritic area.

widely varying in shape and size. The primary dendritic gamma/gamma prime consists of more or less tetragonal gamma prime particles. Also present in the as-cast SX alloy are carbides of the MC type that are rich in Ta and Hf with small amounts of Ti, W and Ni. These particles were found at the interdendritic regions and have irregular plate like cross-sections (Zrnik amd Hornak, 2000). In intermediate regions, between the eutectic pools and the regular gamma/ primary gamma, the carbides were found to be "script-like' (Lukas and Kunz, 2002).

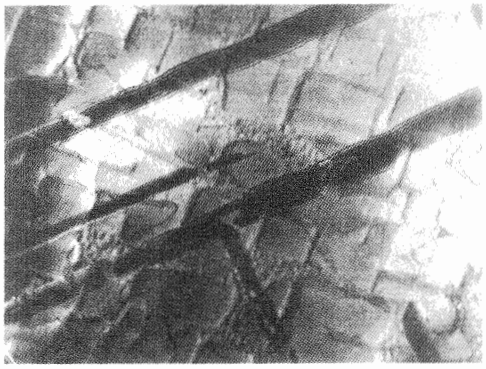

Figure 4 TEM micrograph of gamma prime particles.

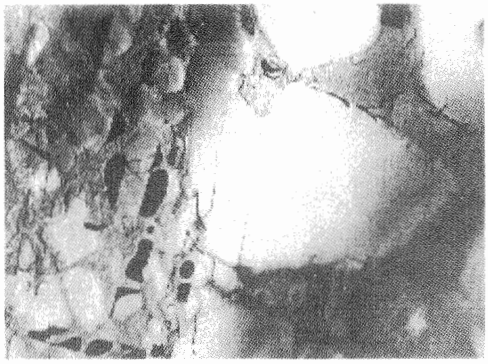

Figure 5 Gamma prime heterogeneity in transient region.

More detail of the as-cast structure was able to be identified by TEM analysis of the thin foils. The homogenous regular tetragonal gamma prime morphology from the secondary dendrite arm is presented in Figure 4. In some of the gamma channels small spherical gamma prime particles are found. The eutectic structure from interdendritic regions, in Figure 5 displays irregular features.

Thermal fatigue

At thermal fatigue tests the temperature-mechanical strain (corresponding to specimen transverse thermal dilatation) depending on the cycle's number have been recorded and analyzed. When heating the specimen to a maximum and cooling it to an initial point temperature, the thermal cycle was completed and a thermal hysteresis loop was recorded. The example of selected deformation loops record from a test of 100 cycles applied is presented in Figure 6.

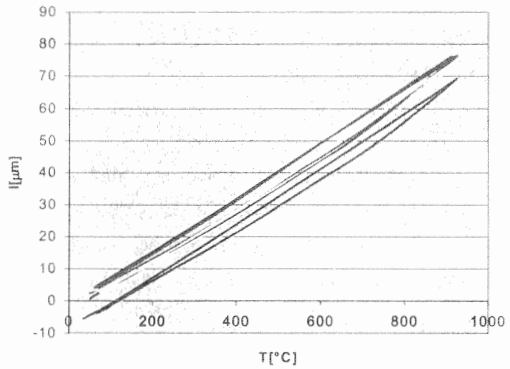

Figure 6 Example of selected dilatation loops from set of 100 thermal cycles applied.

The thermal expansion experimental was carried out to determine the coefficient of thermal expansion. The mean coefficient of thermal expansion for the defined thermal interval of cycling was formulated: $\dot{\alpha} = 14.99 \times 10^{-6}\ K^{-1}$. The coefficient of thermal expansion as a function of temperature was calculated as the polynomial too, and received a formula for the true coefficient of expansion $\alpha_{(T)}$, which was then expressed as follows:

$$\alpha_{(T)} = 1.24*10^{-3}-9.0054*10^{-7}X+5.0423*10^{-9}X^2-7.7134*10^{-12}*X^3+4.6853*10^{-15}*X^4 \quad (1)$$

In order to determine the mechanical strain and thermal stress originating due to thermal transients, the precise analysis of recorded deformation loops, i.e. dependence of transverse specimen dilatation as a function of temperature change, was conducted. The stresses incurred in the specimen are calculated using recorded strains and both coefficients of thermal expansion of SX CM186LC. For the case of stress evaluation in the specimen due to thermal change, the following formula to calculate the stress was employed:

$$\sigma = \dot{\alpha} .E.\Delta T \quad (2)$$

The resonance measurements for given temperature range were performed to identify the elastic constant E of SX superalloy (Fedelich and Beckman, 2002).

Concerning the more precise stress evaluation the differential thermal coefficient of expansion was employed where $\alpha_{(T)}$ varies with temperature. The formula for stress calculation was as follows:

$$\sigma = \{\ln(\Delta l/l_o + 1)/(\alpha_{(T)}.\Delta T)E\} \quad (3)$$

The representative examples of the strain and stress calculated according to equation (2) and (3) for thermal cycles of 10 and thermal interval of 50 – 950 °C are presented in Figure 7 and Figure 8.

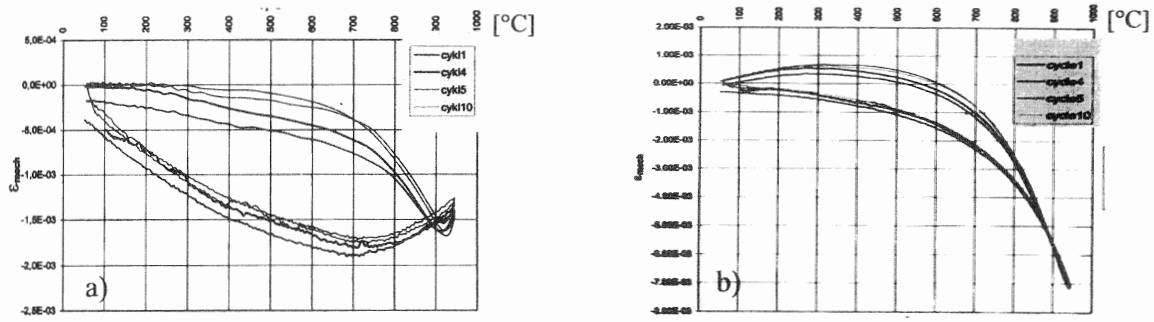

Figure 7 Thermal strain dependence in as-cast specimen exposed to 10 cycles. a) α = const; b) α = f(T).

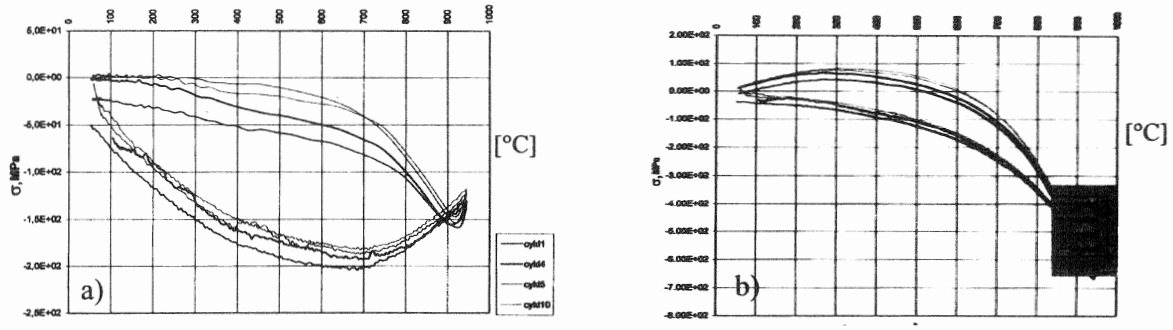

Figure 8 Thermal stress dependence in as-cast specimen exposed to 10 cycles. a) α = const; b) iα = f(T).

Employing the received specimen dilatation data and the modulus of elasticity E data as a function of temperature, the max stress and strain values in individual cycles are available. Concerning the stress evaluation in time of thermal cycle the maximum stress corresponds to the maximum width recorded in each individual dilation loop. The records of maximum stress reached in randomly selected individual thermal cycles after applying a total of 100 cycles are presented in Figure 9. As could be seen from those plots, the maximum stress value was recorded in the temperature region of 400 – 700°C for each chosen specific dilatation loop. However the absolute maximum stress value, regardless of the number of thermal cycles applied in sequence, was detected within the first five cycles. After reaching the maximum value the stress decreases as the continuation of thermal fluctuation proceeded.

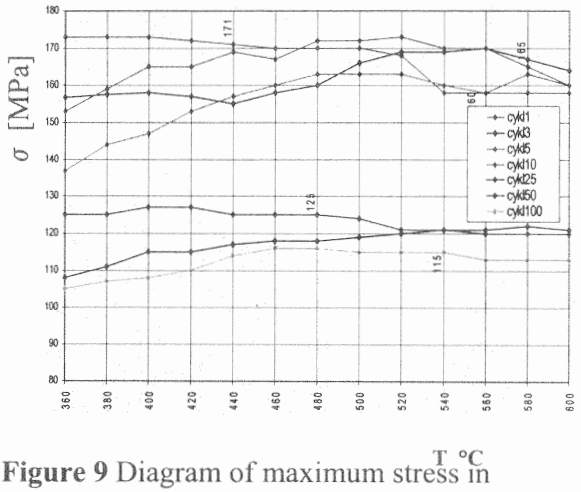

Figure 9 Diagram of maximum stress in specimen resulting from 100 thermal cycles applied.

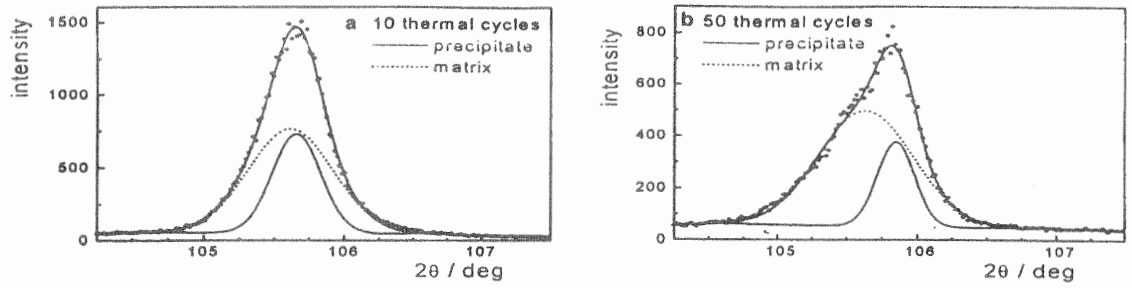

Figure 10 Neutron diffraction profiles of gamma and gamma prime phase resulting from thermal cycling.

Neutron diffraction strain analysis

Concerning the microstrain evaluation originating in the nickel based SX superalloy due to thermal fatigue the high resolution neutron diffraction (HRND) technique has been used. The HRND stress analysis was carried out to the specimens subjected to various numbers of thermal cycles (up to 1000 thermal cycles). The neutron diffraction profiles of the gamma matrix and the gamma prime particles were recorded and analysis of their shape and width provided the information on microstrain state characterisation. The examples of the measured profiles for a different number of thermal cycles applied are shown in Figure 10. The shape of the profiles for gamma matrix and gamma prime particles is described well by Gaussian distribution and the distance between the corresponding peaks gives the constrained misfit between these two phases at each thermal cycle (as opposed to the unconstrained misfit which is present in the virgin alloy), figure 11. The initial state of material is characterized by phase specific microstrains resulting from elastic stresses between gamma matrix and precipitates. The observed constrained misfit is negative and of relatively

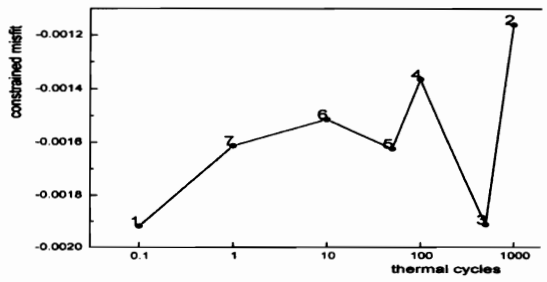

Figure 11 The evolution of the constrained lattice misfit.

small value (~19 x 10^{-4} for reference state). The microstrain in gamma matrix and gamma prime precipitates started to increase immediately after the first were introduced. For thermal cycling with a higher number of cycles in test the micro strain values showed scattered dependence. For the as-cast SX CM186LC superalloy, the evolutions of constrained misfit, as well as that of the root-mean-square microstrain values extracted from the diffraction profiles, has been difficult to interpret after around fifty cycles. This difficulty can be attributed to the heterogeneity of the dendritic and interdendritic microstructure as well as the large volume content of the eutectic. The investigation of the fully solutioned SX CM186LC superalloy with the additional objective to show that the problems experienced with the as-cast variant are the direct consequence of the microstructural heterogeneities.

CONCLUSION

The single crystal nickel based superalloy CM186LC was evaluated in a thermal fatigue response according to laboratory conditions. The following conclusion can be drawn from received results:

- In consequence of thermal cycling the relatively high stress was originating in specimen already after the first thermal cycles were introduced.
- As cycling continued the maximum value of stress was detected for the first five cycles. For more advanced thermal cycling the decrease in stress was observed.
- The neutron diffraction technique was useful to microstrain analysis in exposed specimens. It revealed that thermal fluctuation could nucleate the stress originating due to an increasing lattice mismatch of phases the alloy consists of as the number of thermal transients increases.
- An irregularity in microstrain dependence was observed. The appearance of the abrupt fall down in the strain for a higher number of thermal transients is difficult to bring a reasonable explanation, but it can be a consequence of the microstructure heterogeneity of as-cast alloy.

REFERENCES

Blumm, M., Meyer-Olberslegen, F. and Rézai-Aria, F. 1995. *Fatigue under Thermal and Mechanical Loading,* London, Kluwer Academic Publ.: 13.

Cyrska-Filemonowicz, A. and Dubiel, B. A. 2000. *Annual Report COST522, Project No. PL 101.* AGH Cracow.

Fedelich, B. and Beckman, J. 2002. *Annual Report COST 522, Project No.D 103.* BAM –Division V.2 Berlin.

Kasik, N., Meyer-Olbersleben, F., Rézai-Aria, F., Blumm, M. and Ilschner, B. 1998. *Proc. of the 6th Liege Conference on Materials for Advanced Power Engineering, Liege* : III-1357.

Lukaš, P. and Kunz , L. 2002. *Annual Report COST 522, Project No. CZ101.* IPM ASCR Brno.

Lukas, P., Zrnik, J., Ceretti, M., Vrana, M., Mikula, P., Strunz, P., Neov, D. and Keuerleber, J. 1998. *Proc. of the 6th EPDIC Budapest* : 244.

Malpertu, J. L. and Remy, L. 1990. *Met. Trans. A.* **21A (2)** : 389.

Zrnik, J. and Hornak P. 2000. *Annual Report COST 522, Project No. SR 101.* TU Košice.

(Revised version accepted February 23, 2004)